scientific reports

Check for updates

OPEN

Unlocking the potential of the terrestrial gastropod species *Zootecus insularis* as a climate archive for arid regions

Katharina E. Schmitt[1,12]✉, Lucas Proctor[2,3,12]✉, Tara Beuzen-Waller[4], Conrad Schmidt[5], Susanne Lindauer[6], Mathilde Jean[7], Maria P. Maiorano[8], Martin Sauvage[9], Jennifer Swerida[10], Dana Pietsch[11] & Bernd R. Schöne[1]

Local-scale climate reconstruction in arid regions is challenging due to the scarcity of suitably preserved archives. While several well-studied climate proxy datasets exist for southeastern Arabia, including those preserved in speleothems, sedimentary deposits and paleosoils, and occasionally sediment cores collected for pollen analysis, snails have not yet been explored as a potential archive. This study investigates the potential of the terrestrial gastropod *Zootecus insularis* collected from geoarchaeological sections as new climate archive for arid environments. Isotope analysis was conducted on specimens from Holocene contexts in Oman to reconstruct long-term climate trends. Previously published water temperatures calculated from oxygen isotope data of *Melanoides tuberculata*, a freshwater gastropod species found in the same geoarchaeological sections as the terrestrial *Zootecus* shells, were interpolated to the age of the terrestrial snails, allowing for the recalculation of an oxygen isotope signal used to identify wet or dry periods. The resulting dataset showed a strong correlation with existing paleoclimate datasets from speleothems and paleolakes. Additionally, the $\delta^{13}C$ values of *Z. insularis* indicated a significant shift towards more negative values over time, which probably suggests a transition from C4 grass-dominated vegetation to mixed C4/C3 xerophilic vegetation. This integrated approach suggests that snails could provide a valuable new archive for paleoclimate studies in arid regions.

Keywords Paleoenvironmental reconstruction, Stable isotopes, Climate proxy, Vegetation change, Drylands

A common challenge for paleoclimate reconstruction in dryland regions is finding suitable climate archives that record rainfall variability and the correlative responses of ecosystems more or less continuously. Despite the availability of several records of continental archives for reconstructing Quaternary hydro-climatic fluctuations in southeastern Arabia, including high-resolution oxygen isotope profiles from speleothems[1–6], aeolian formations[7–10], fluvial formations[11–14], paleosoils[15–17], lacustrine/sabkha sediments and microfauna[18,19], phytoliths[20,21], and occasionally pollen records[15,20–25] most of those archives are site-specific, hence very heterogenous in their formation and preservation.

[1]Institute of Geosciences, University of Mainz, Johann-Joachim-Becher-Weg 21, 55128 Mainz, Germany. [2]Department of Sociology, Anthropology, and Criminal Justice, Utah State University, Old Main 245, Logan, UT 84321, USA. [3]Institute for Archaeological Science, Goethe University Frankfurt, Norbert-Wollheim-Platz 1, 60629 Frankfurt am Main, Germany. [4]Université de Perpignan Via Domitia, Histoire naturelle de l'Homme préhistorique (HNHP), UMR 7194 CNRS, UPVD 52 Avenue Paul-Alduy, 66860 Perpignan, France. [5]Institute for Ancient Near Eastern Studies (IANES), University of Tübingen, Burgsteige 11, 72070 Tübingen, Germany. [6]Curt Engelhorn Center Archaeometry gGmbH, 68159 Mannheim, Germany. [7]Department of Scientific Research, The British Museum, Great Russell Street, London WC1B 3DG, UK. [8]Institue of Archaeology, Czech Academy of Sciences, Letenská 4, 118 00 Prague 1, Czechia. [9]CNRS, UMR 7041-ArScAn/VEPMO, UMR 7041 ArScAn/VEPMO, MSH Mondes, bât. Ginouvès, 21allée de l'Université, 92023 Nanterre Cedex, France. [10]Department of World Archaeology, Leiden University, Einsteinweg 2, 2333 CC Leiden, The Netherlands. [11]Chair of Soil Science and Geomorphology, University of Tübingen, Rümelinstr. 19-23, 72070 Tübingen, Germany. [12]Katharina E. Schmitt and Lucas Proctor contributed equally to this work. ✉email: Katharina.schmitt@uni-mainz.de; lucas.proctor@usu.edu

Quaternary rainfall variability in Arabia is driven by both meridional and zonal displacements of the Intertropical Convergence Zone (ITCZ) and shifts in the northward extent of the African and Indian summer monsoon. These processes have, in the past, transformed the Arabian Desert into a savannah-like landscape with numerous lakes and wetlands[4], e.g., during the Holocene Humid Period (ca. 10.1–6.3 ka BP), which alternated with dry periods caused by the shift from summer monsoonal to winter-dominated rainfall regimes[2,4–6,21].

This study explores the potential of the terrestrial snail *Zootecus insularis* as a new archive for climate reconstructions in arid regions, such as southeastern Arabia, where traditional archives are scarce or poorly preserved. The snails are of particular interest as they can offer insights into both long-term climate trends (combining all snails) and short-term events (examination of single shells). The 85 specimens used in this study were collected from Holocene stratigraphic layers, sampled for high-resolution isotope ratio mass spectrometry (IRMS) measurements, and then age-dated as part of the UmWeltWandel project (Fig. 1). These snails are widespread, have limited mobility, and are sensitive to environmental fluctuations. Moreover, their shells are resilient to degradation over time, making them valuable as both long-term paleoenvironmental indicators and records of short-term events such as localized rainstorms[26–32]. To assess the reliability of this approach, the $\delta^{18}O_{water}$ values derived from 85 terrestrial snail specimens were compared with the established speleothem, lacustrine and vegetation records from southeastern Arabia. Additionally, their $\delta^{13}C_{shell}$ values indicate a change in vegetation over time, possibly representing a decline in overall availability of C4 plants on the landscape. As the first study combining aquatic and terrestrial snail data for paleoenvironmental reconstruction, the objective of this analysis was to provide insights into vegetation dynamics and climate variability in the southern Al-Hajar piedmont and raise important methodological questions requiring further study.

Results

Shell stable oxygen isotopes

The high-resolution $\delta^{18}O_{shell}$ dataset of *Z. insularis* ranged from - 11.1 to + 11.5 ‰, covering the time interval of 13.5 ka BP to the present. Of the 85 snails, a total of 31 were classified as Types 2 A–C and E, corresponding to event signals (Fig. 2, squares), based on Schmitt and Beuzen-Waller et al.[31]. These event types include (A) strongly evaporative patterns, (B) continuous freshwater inputs, (C) meteorological events, and (E) fast wet/

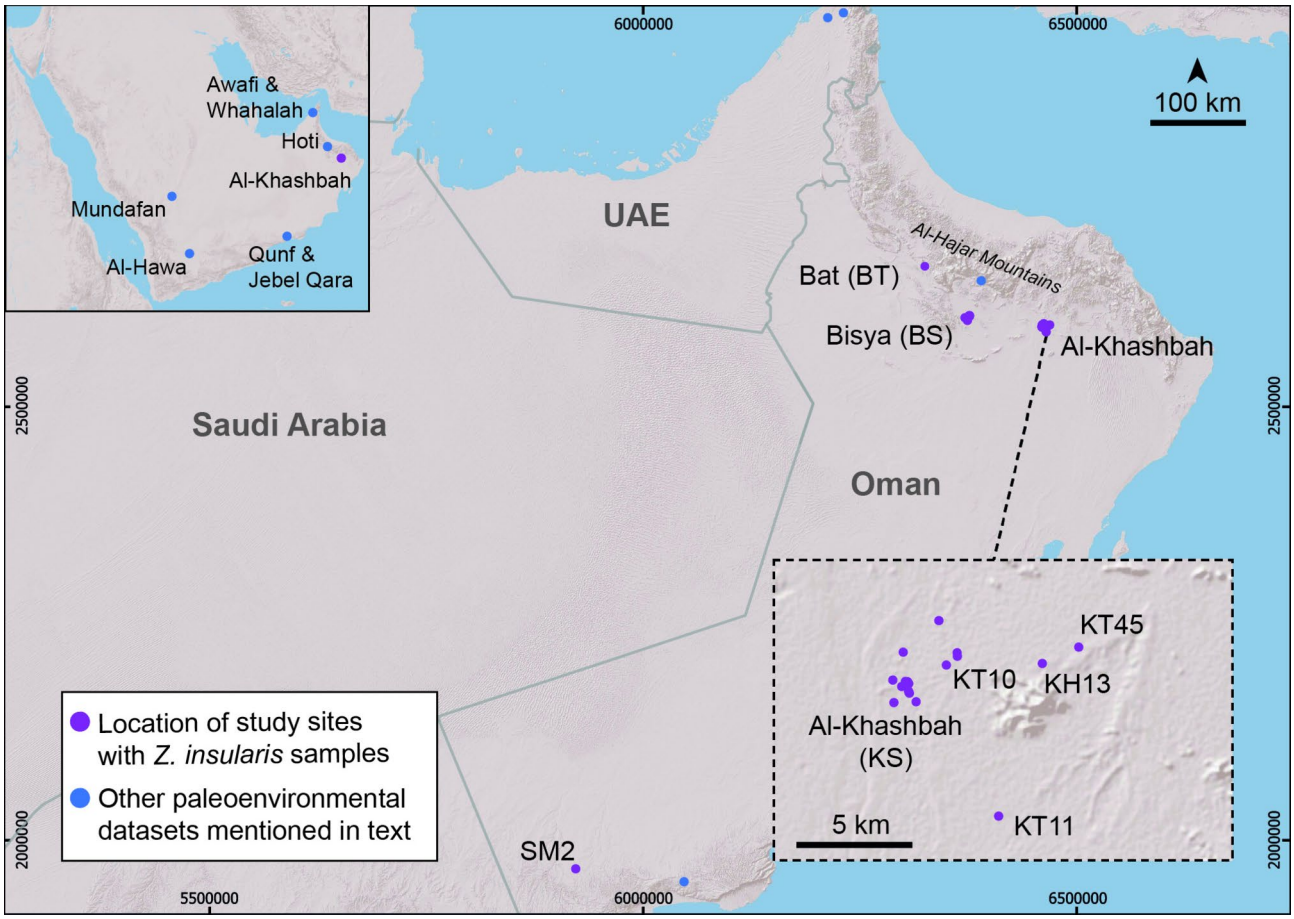

Fig. 1. Geographical overview of the sampled sites analyzed in this study, most of which were collected in the vicinity of the town of Al-Khashbah. Map scale is presented in metres and projected in UTM40N. The locations of other published paleoenvironmental studies from the region mentioned in the text are presented for comparison. The inset depicts the concentration of sampling in the immediate vicinity of Al-Khashbah.

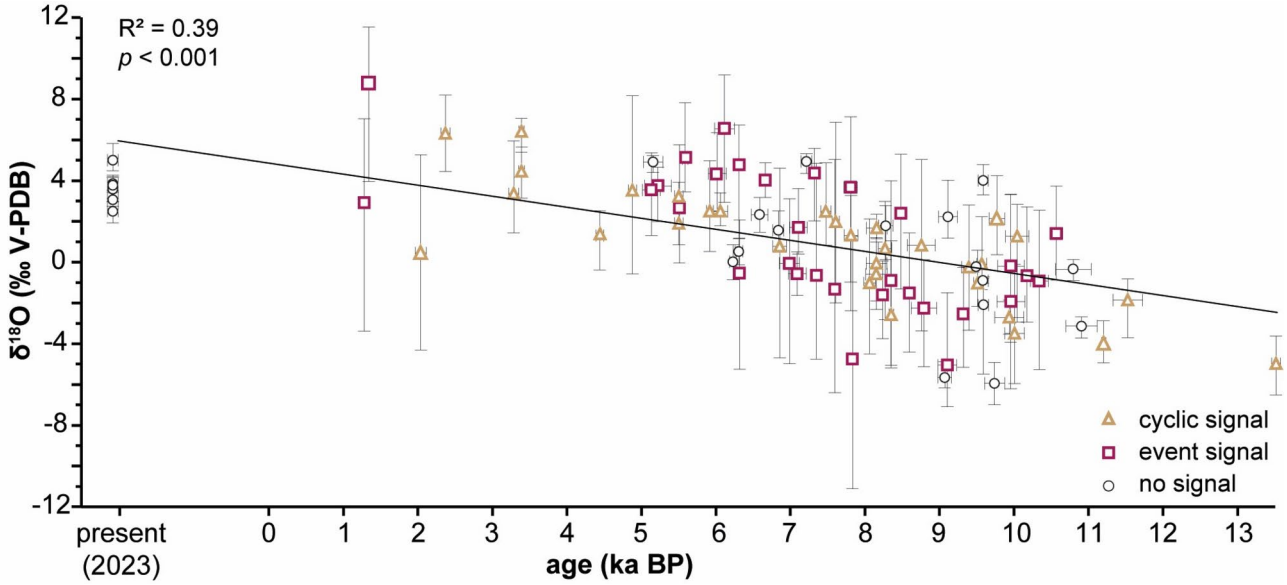

Fig. 2. Summary of all stable oxygen isotope data plotted against their age (ka BP). Please note: the radiocarbon ages in the graph are calibrated (see Ref.[39]; S41) and are presented here as calendar ages in ka (1000 years) BP. Triangles represent individuals recording cyclic $\delta^{18}O_{shell}$ patterns, squares events and circles were snails where no pattern could be identified. The error bars of each value indicate the age range (2σ, horizontal) and the range of $\delta^{18}O_{shell}$ values (vertical).

dry cycles. A cyclical pattern (alternating evaporative and freshwater input conditions), classified as Type 2 D, was observed in 32 snails (Fig. 2; triangle). Due to limited data, the remaining snails were not assigned to a pattern (Fig. 2; circle). Both event-based signals and cyclical signals are distributed across the entire studied time interval. A discernible upward trend is evident, with an increase of + 8.1 ‰ over time (R2 = 0.39; $p < 0.001$). For a more detailed description please refer to "Classification of the high-resolution shell data".

Shell stable carbon isotopes

The high-resolution $\delta^{13}C_{shell}$ dataset from the analyzed terrestrial snails ranges from - 10.9‰ to + 1.1‰ (Fig. 3). A discernible negative trend was evident, with a decrease of the $\delta^{13}C_{shell}$ values over time by - 8.5‰ (R2 = 0.40; $p < 0.001$).

Discussion

Comparison of snail-derived environmental data with established climate archives

Despite Oman having only two primary moisture sources, determining the origin of precipitation from terrestrial snail-derived $\delta^{18}O_{water}$ values proves challenging as the snail $\delta^{18}O_{water}$ values span - 2.9‰ to + 7.5‰, encompassing both moisture sources (Mediterranean Sea: $\delta^{18}O$ = - 4.5 to + 1 vs. Indian Ocean: $\delta^{18}O$ = - 10 to - 2‰)[4,34,35]. This broad range reflects the inclusion of the minimum and maximum $\delta^{18}O_{shell}$ values. To interpret the calculated $\delta^{18}O_{water}$ values, the classic assumption of the "amount effect"[36] was modified and applied: High $\delta^{18}O$ values indicate drier conditions with reduced monsoonal (winter-spring) precipitation, while lower $\delta^{18}O$ values suggest wetter conditions, typical of a monsoonal (summer) rainfall regime[2,4,6,33,37,38]. While quantitative data are lacking, isotopic variations qualitatively reflect past climate shifts between wetter and drier periods (Fig. 4).

To mitigate the impact of extreme events, a 10-point average was applied to the snail $\delta^{18}O_{water}$ values, revealing seven distinct phases (I–VII) (for detailed measurements, please refer to[39], and for a complete explanation of the methodology, please refer to 4.8–4.10). These phases were compared to established paleoclimate records from the Arabian Peninsula to assess the reliability of this new archive. These comparative records include $\delta^{18}O$ values from speleothems of the Hoti Cave (~ 80 km west of Al-Khashbah)[2,6] and the Qunf Cave (~ 900 km south of Al-Khashbah)[1], lacustrine records from the palaeolakes of Awafi and Wahalah (UAE)[15,20] and Al-Hawa (Yemen)[23], as well as vegetation data from Mundafan (Saudi Arabia) and Jabal Qara (Oman)[33].

(I) 10.2 to 9.6 ka BP: This time interval is marked by low $\delta^{18}O_{water}$ values (+ 0.4 ± 1.8‰), suggesting a generally humid phase interrupted by two short arid episodes (~ 10.1 and 9.8 ka BP), indicated by positive $\delta^{18}O_{water}$ excursions. Al-Hawa's lacustrine record points to a dry phase (10.5–10.1 ka BP), followed by a wetter phase (10.1–9.1 ka BP)[23]. Records from Jabal Qara indicate a wet period with a "savannah-like environment," based on the presence of a large concentration of deposited terrestrial gastropods[33].

(II) 9.6 to 8.1 ka BP: A significant rise in $\delta^{18}O_{water}$ values (up to + 4.5‰) signals a transition to drier conditions, punctuated by a brief wet period between 9.1 and 8.9 ka BP. Positive peaks at 9.2 ka BP (+ 2.8‰) and 8.2 ka BP (+ 4.5‰) align with positive excursions in the Hoti Cave speleothem record[2], though such

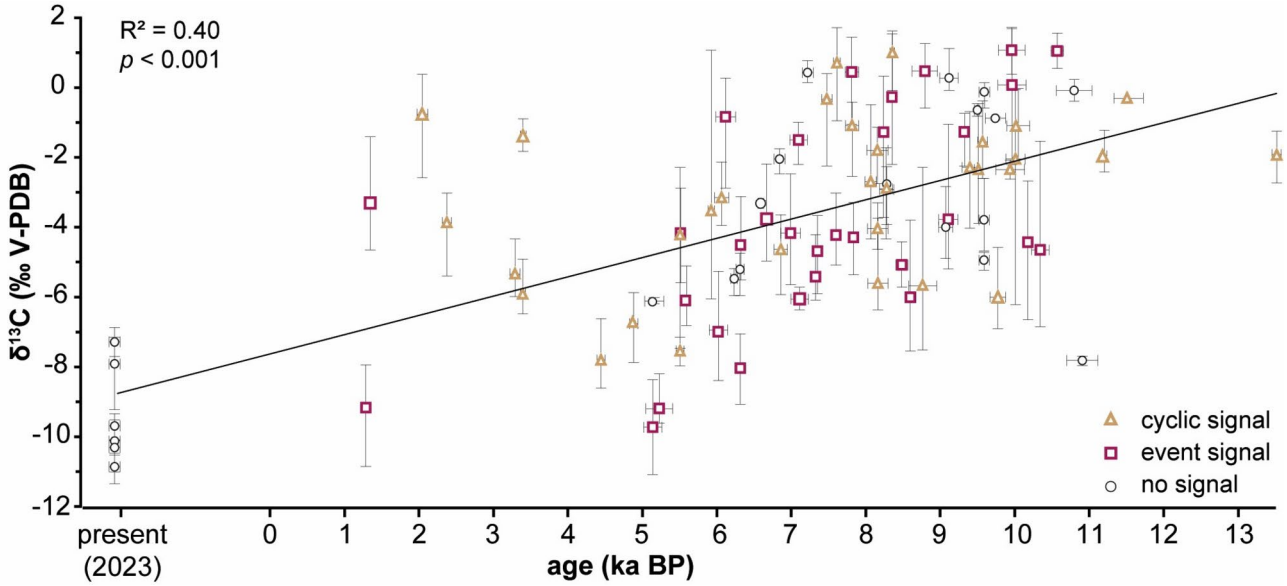

Fig. 3. Summary of all stable carbon isotope data plotted against time (ka BP). Please note: the radiocarbon ages in the graph are calibrated (see Ref.[39]; S41) and are presented here as calendar ages in ka (1000 years) BP. The error bars of each value indicate the dating uncertainty (2σ, horizontal) and the range of the $\delta^{13}C_{shell}$ values (vertical).

peaks are absent in the Qunf Cave[1]. Several positive excursions between ~ 9.5 to 9.1 ka BP in the Hoti Cave suggest a drier environment, followed by wetter conditions after 9.1 ka BP. Lacustrine records from Al-Hawa (Yemen) also indicate a dry phase after 9.1 ka BP[23].

(III) 8.1 to 7.4 ka BP: $\delta^{18}O_{water}$ values decrease from + 4.5‰ to + 2.6‰, reflecting a wetter climate. This shift aligns with the Hoti Cave speleothem record, where $\delta^{18}O$ values drop after peaking around 8.1 to 8.0 ka BP[2,6]). Similarly, lacustrine phases at Al-Hawa (8.4–8.0 and 7.8–7.5 ka BP) suggest wet conditions, punctuated by a dry phase[23]. However, short-term aridity events at Awafi (7.9 and 7.6 ka BP)[15] and a transition to drier conditions at Wahalah (7.7 ka BP)[21] contrast the recorded wetter conditions from the speleothems and the snails.

(IV) 7.4 to 7.1 ka BP: An increase in the $\delta^{18}O_{water}$ values to + 3.8‰ points to increasing aridity. This transition is mirrored in the Wahalah lake sediments[21] and in the Hoti Cave speleothem data, where two positive excursions in the $\delta^{18}O$ values are recorded[2].

(V) 7.1 to 6.4 ka BP: The $\delta^{18}O_{water}$ values (+ 3.6 ± 0.2‰) suggest a relatively stable climate, with drier conditions according to the relatively high $\delta^{18}O_{water}$ values. This is confirmed by the Hoti Cave record, where two positive excursions are visible.

(VI) 6.4 to 6.2 ka BP: A sharp drop in the $\delta^{18}O_{water}$ values to + 2.7 ‰ is indicative of a rapid transition to wetter conditions. Conversely, the Hoti Cave speleothem record shows a sharp shift to drier conditions (higher $\delta^{18}O$ values) starting from 6.3 ka BP[6].

(VII) 6.2 ka BP to present: Although snail data are limited for more recent periods, an upward trend up to + 4.8‰ was recorded, suggesting a (steady) transition to a drier climate, which is consistent with other data: Speleothem data from Hoti Cave show a positive excursion (~ 5.5 ka BP), and Awafi lake sediments record an arid phase (5.9–5.2 ka BP)[15].

In conclusion, the snail-derived water isotope dataset aligns very well with the established paleoclimatic record from speleothems, lakes, and vegetation. Deviations in the duration of humid/dry periods, such as during phases III or IV, may result from differing response times and formation processes among these archives and geographic factors. For instance, speleothems are sensitive to microenvironmental variations within caves[40] and cease growing under unfavorable conditions. Similarly, snails enter aestivation, halting environmental recording, and may experience metabolic effects that influence isotopic signals[41] while lacustrine deposits consistently provide a precipitation-evaporation record caused by environmental changes in that area[38].

$\delta^{13}C_{shell}$ pattern and vegetation shift

In addition to providing paleoclimate information, this dataset provides a new record of vegetation change over time for the southern Al-Hajar piedmont zone. Owing to a variety of preservation issues caused by aridity, aeolian erosion, and/or sparse vegetation cover, long-term Holocene vegetation reconstructions using traditional proxies (e.g., sediment cores collected for pollen analysis, archaeobotanical reconstructions) for the study area are scarce.

Previous studies of land snail shells have demonstrated that their carbon isotope composition largely reflect the relative proportion of C3 and C4 vegetation of the region in which the organism lived, provided several factors are

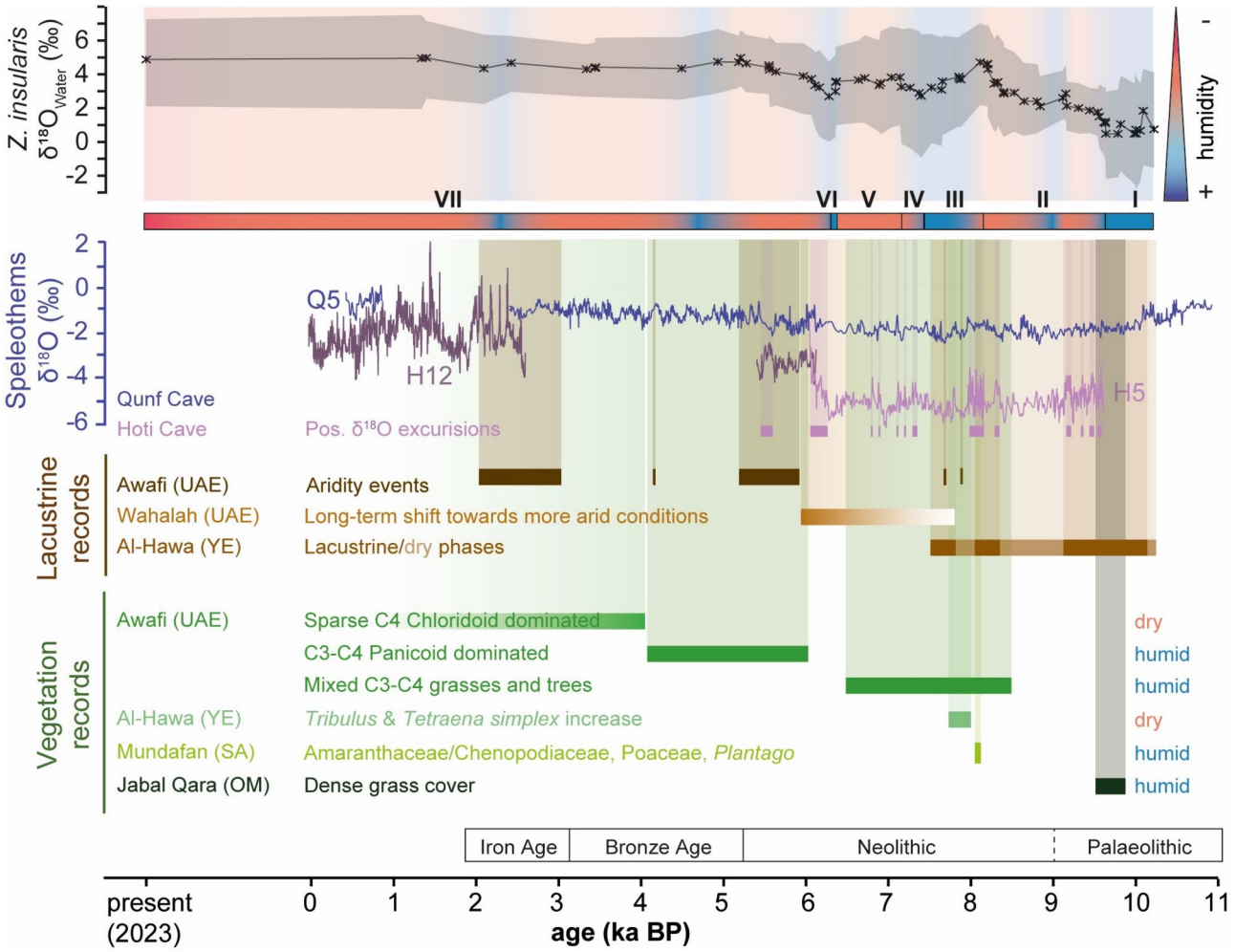

Fig. 4. A 10-point average $\delta^{18}O_{water}$ curve was calculated from the individual $\delta^{18}O_{shell}$ values (crosses) of the terrestrial snail and was divided into seven sections (I–VII). The shaded area in the figure represents the calculated minimum and maximum values of the individual snails. Data from Hoti Cave were derived from Fleitmann et al.[2,3] and Neff et al.[6], while those from Qunf Cave were taken from Tian et al.[1]. Lacustrine records originated from Awafi[15] and Wahalah[21] lake records in the United Arab Emirates as well as Al-Hawa Lake in Yemen[23]. Vegetation data are from Jabal Qara (Oman)[33], Awafi[15,20] and from Al-Hawa and Mundafan in Saudi Arabia[24]. Archaeological periods were adapted and simplified from Beuzen-Waller et al.[12].

considered[42–46]. The carbon isotope signal of terrestrial gastropod shells is derived mainly from dietary sources. Snails feed on plant matter and surface detritus resulting from local vegetation communities. Several factors have been suggested to cause variability in $\delta^{13}C_{shell}$ values. Following consumption, metabolic processes result in a systematic $\delta^{13}C_{shell}$ increase of over 8 ‰ compared to the dietary carbon sources, provided the shell was formed in isotopic equilibrium[43]. Further alteration of the original carbon signal may occur through local variations in CO_2 concentrations and the consumption of soil carbonates by individual snails. While organic carbonates are thought to reflect a time-averaged signal of local vegetation composition, inorganic soil carbonates tend to be more enriched in ^{13}C than C3 vegetation[46], potentially leading to an increased offset in $\delta^{13}C_{shell}$.

The data in this study show a steady decrease in the $\delta^{13}C_{shell}$ values over time (Fig. 5). At first glance, these results suggest a progressive decline in the proportion of C4 plants, which runs counter to current available regional reconstructions from across southeastern Arabia. At Awafi (UAE), for example, an overall positive shift (ca. 2–3‰) of $\delta^{13}C$ data from sedimentary carbon was reported for over the course of the middle and Late Holocene[20]. According to these authors, this observation, combined with corresponding data from pollen and phytolith results, was indicative of a transition from mixed C3–C4 grassland to C4-dominated vegetation in the region. Today, the modern vegetation at Awafi is broadly similar in composition to the Al-Khashbah area. Qunf Cave[1], located far to the south in the Dhofar Mountains, recorded a relatively stable $\delta^{13}C$ in speleothems until ca. 3 ka BP, though interpreting single speleothem records is complex as they can be moderated by a range of variables including type/density of vegetation, water source, and cave atmosphere[42].

One possible explanation is that the trend towards lower $\delta^{13}C_{shell}$ values reflects a decline in the proportion of available biomass from seasonal C4 xeromorphic grasslands associated with hot, humid summer precipitation[47] as the ITCZ shifts southward at the end of the Holocene Humid Period. As summer rainfall decreased, these

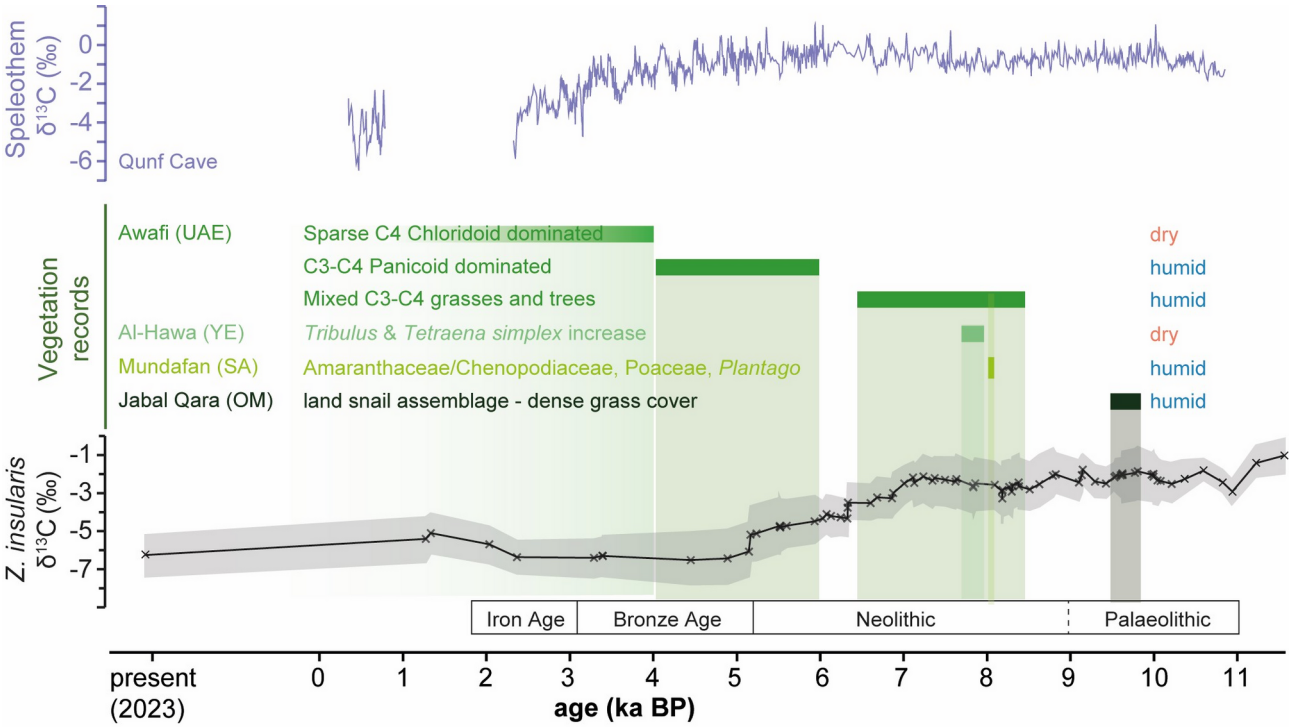

Fig. 5. 10-point average of $\delta^{13}C_{shell}$ plotted alongside published regional paleo-vegetation records derived from Jabal Qara[33], Awafi[20], and at Al-Hawa and Mundafan[24]. Speleothem $\delta^{13}C$ data from Qunf Cave[1] are provided as a reference. Archaeological periods are adapted and simplified from Beuzen-Waller et al.[12].

rapid-growing grasses would appear on the landscape for fewer days per year and therefore contribute less to the overall snail diet. Meanwhile, C3 perennials and xerophilous C4 plants (e.g., Chloridoid, eudicots including Amaranthaceae, etc.), would have remained throughout the year. Such a pattern would reflect the same transition observed in the pollen and phytolith data from Awafi[20], albeit beginning several thousand years earlier.

An alternative hypothesis for the $\delta^{13}C$ results is that the negative shift in $\delta^{13}C_{shell}$, particularly at the Neolithic-Bronze Age transition, represents the emerging impact of human activity through the cultivation of C3 crops. The nature and timing of the development of proto-oasis cultivation in this region remains under debate[48], and evidence for agricultural production at the beginning of the Bronze Age, particularly in the vicinity of Al-Khashbah[49,50], is limited. Furthermore, this interpretation fails to account for the decline in $\delta^{13}C_{shell}$ during the Neolithic, from 7000 BP onwards. While human activity is attested in the study area during this period[51], this appears to have been limited to relatively low-impact hunter-pastoral mobile campsites, unlikely to significantly alter vegetation.

In summary, $\delta^{13}C_{shell}$ data indicate a transition of local vegetation composition in the southern Al-Hajar piedmont beginning ca. 7000 BP. While carbon isotope data from shells represent an overall signal of local vegetation, untangling the complexities of C3/C4 plant communities from such data is challenging without the addition of palaeobotanical datasets. Limited archaeobotanical studies from this region provide limited data in support the retention of open woodlands following the onset of aridity. Charcoal data from Bat and Al-Khashbah suggest little change in the overall composition of woody vegetation between the Neolithic and Bronze Age[49,50]. However, further research on long-term vegetation succession of the southern Al-Hajar piedmont is essential to refining interpretations of this dataset.

Limitations and areas of future research

As demonstrated in Fig. 4, calculating the isotopic composition of water consumed by snails offers valuable insights, making them a potential archive for long-term climate reconstruction. However, several factors need to be investigated further before fully utilizing snails as a new climate proxy: Life span and modern-process studies: The rate of shell formation and, consequently, the animal's life span are not known due to the indistinctness of the growth lines. However, it can be hypothesised that a correlation exists between size of shell and longevity. Moreover, the absence of any living snail in this project precluded the utilization of uniformitarianism. For a detailed discussion of this topic please refer to Schmitt & Beuzen-Waller[31]. Transport: Snail shells can be relocated both vertically and horizontally by natural forces like rainfall and rivers[52]. However, this post-mortem transport is usually over short distances, as long-distance movement due to strong flash floods would likely destroy the shell[31]. Since this study focuses on long-term climate trends rather than specific stratigraphic contexts, the transport issue is considered less critical for the dataset used here. Age dating: Determining the precise age of snail shells is challenging, particularly when affected by a possible "hardwater effect"[53,54]. This effect can result in significant dating errors, ranging between 1000 to 3000 years[53]. Consequently, potential

time discrepancies concerning climate conditions may occur, and further research on this topic is required. Diagenetic alteration: Diagenetic alteration, especially in aragonitic shells, is a concern for isotopic studies. However, Raman spectroscopy analysis showed that the snail shells analyzed here are unlikely to have undergone significant alteration, implying good preservation[31]. Limitations of modeling: Two key parameters govern the $\delta^{18}O_{water}$ values, namely $\delta^{18}O_{groundwater}$ and temperature. In Oman, $\delta^{18}O_{groundwater}$ varies considerably, from - 3.7‰ to + 0.5‰[55], largely due to differing recharge altitudes[35] and the two distinct moisture sources. Despite these variations, the groundwater isotope composition in arid regions has been shown to remain stable over long intervals of time[34,35]. A mean $\delta^{18}O_{water}$ value based on collected field data (2022/2023) was used but this value may fluctuate depending on which aquifer is used. As this study represents the first attempt to apply snail shells as long-term climate archives, this parameter may be adjusted in future studies. Furthermore, the calculated temperatures derived from the aquatic *M. tuberculata* snails and interpolating them to the ages of the terrestrial snails may introduce discrepancies in the $\delta^{18}O_{water}$ signal. While we can reasonably assert that the aquatic snails classified as Type 1 A and B likely inhabited groundwater[31] and recorded therefore the ambient air temperatures, this approach presents another potential source of error. Nevertheless, modifying these two parameters will not alter the overall pattern; while the values may fluctuate, the pattern itself will remain consistent.

Material and methods

Project description and study area

The modern village of Al-Khashbah (Oman) is located in the southern piedmont of the Al-Hajar Mountains, at the western border of the Ash-Sharqiyah North governorate. This study draws upon material collected from both archaeological excavations and geomorphological soundings conducted in its vicinity, between 2016 and 2023 as part of the UmWeltWandel joint research project[31,56] and the University of Tübingen excavations at Al-Khashbah[57,58].

Al-Khashbah features a rich archaeological landscape with hundreds of identified features across the region, demonstrating near continuous visitation and/or inhabitation from the Neolithic (ca. 8000 BP) onwards[51,59,60]. A substantial Early Bronze Age occupation developed in Al-Khashbah during the Hafit and Umm an-Nar periods (ca. 5250–3950 BP). Survey and excavations at the site have identified at least nine monumental buildings, numerous tombs, the earliest evidence for copper production in Oman[57–59], scattered Middle–Late Bronze Age and Iron Age remains[59,60], and several abandoned oasis settlements from the last 500 years[61].

The UmWeltWandel Project was established in 2020 to conduct interdisciplinary paleoenvironmental analysis in the region as a means of contextualizing local human-environmental relationships, with a particular emphasis on the Early Bronze Age occupations at Al-Khashbah. Soundings were made throughout the area (Fig. 1) to reconstruct the evolution of the local wadi system through the Holocene[31].

Today, the region is characterized by a hot, arid climate, with a mean annual temperature of 27.6 °C and mean annual precipitation of 54.1 mm/year (Ash Sharqiyah: 1991–2020)[62]. The area lies outside the orographic influence of the Al-Hajar Mountains and is characterized by both active and relict wadi systems, gravel plains, and low-elevation hills.

The local vegetation belongs to the drought-deciduous *Euphorbia larica-Acacia* (*Vachellia*) *tortilis* open woodland[63,64] found throughout the southern foothills of the Al-Hajar Mountains. It is characterized by mixed C3/C4 scrubland and low-density woodlands growing near wadi beds and recent relict wadi terraces. The woodland component consists of trees belonging to Sahelian vegetation communities, including acacias (*Vachellia tortilis* (Forssk.), Galasso & Banfi and *Vachellia flava* (Forssk.), Kyal. & Boatwr., *Prosopis cineraria* (L.) Druce, and *Maerua crassifolia* Forssk., while *Ziziphus* spp. and *Tamarix* spp. can be found growing along active wadi channels and in moist depressions. Low lying shrubby and herbaceous plants include a mix of C3 and C4 plants including various chenopodiaceous shrubs, *Tetraena qatarensis* (Hadidi) Beier & Thulin, *Rhazya stricta* Decne., *Fagonia indica* Burm.f., *Lycium shawii* Roem. & Schult., *Euphorbia larica* Boiss., *Leptadenia pyrotechnica* (Forssk.) Decne, and others. Grasses and other annuals are uncommon throughout most of the year but include a relatively high proportion of C4 types[49], including *Panicum, Cynadon, Sporobolus,* and *Stipagrostis*. However, after large rainfall events, widespread stands of quickly-maturing grass can appear. Finally, local oases have a mix of C3 crops and field weeds (including wheat, barley, fruit trees, various leafy vegetables, and legumes), and C4 crops (sorghum and maize).

Fieldwork

Snails were collected over the course of three field seasons, during which geoarchaeological sections were opened for the purpose of investigating and dating the various phases of alluvial accumulation and erosion that occurred within local wadi systems throughout the Holocene. Snails from these sections were collected by hand or from flotation samples taken from recorded stratigraphic contexts. A detailed description of the stratigraphy, the position of the snails in the profiles, and their ages have been previously published in an open access data repository[39].

Zootecus insularis

Terrestrial snails like *Zootecus insularis* typically secrete their aragonitic shell for only a few hours per night[65], when the humidity (between 75 and 95%) and the temperature (between 7 to 27 °C) are in an optimal range[49].

Z. insularis has been found in a variety of environments, including agricultural fields, shady trees, small thick bushes, banks of shady canals, sewage ponds[66], mountain gravel plains (up to 1900 m above sea level), premontane environments[67], narrow coastal plains, silty soils between rocks, and vegetation on mountain slopes[52]. It is typically found among the shallow roots of mountain plants, suburban lawns and gardens, parks, and agricultural fields, including *Vachellia* spp., *Prosopis cineraria*, *Ziziphus spina-christi*, *Tamarix*, *Euphorbia larica*, *Helianthemum lippii,* and *Cymbopogon*[52,67–70]. They prefer moist soil with a moderate amount of humus[67]

and can dig to a depth of 25 cm[70]. These snails are restricted to semi-arid habitats and have not been recorded in humid mountains or deserts[71]. *Z. insularis* enters aestivation during prolonged periods of aridity, yet becomes active rapidly following precipitation events[52].

Sample preparation

A total of 85 specimens of the terrestrial snail *Z. insularis* were collected from 27 geoarchaeological soundings throughout north central Oman, largely in the vicinity of Al-Khashbah. The selected shells were freed from dirt and debris by mechanical cleaning. Each shell was placed in an Eppendorf cylinder with deionized water and shaken for 24 h on a shaking table. Specimens were then repeatedly washed in an ultrasonic bath and dried in the oven at 30 °C overnight. Following cleaning, shells were macroscopically checked for the absence of abrasion, fractures, and other conspicuous features that may indicate diagenetic overprinting.

Raman spectroscopy

The shells were analyzed for diagenetic alteration using Raman spectrometry. Six measurements were taken per snail at randomly selected locations to cover a large area[39]. Raman measurements were performed at room temperature using a Horiba Jobin Yvon LabRam spectrometer equipped with an Olympus BX41 optical microscope at the Institute of Geosciences, University of Mainz. A Nd:YAG laser with a wavelength of 532.21 nm, 400 µm confocal hole, 1800 grooves/mm grating, 100 µm entrance slit width and 50 × objective was used. Data were recorded with a 5 s temporal and analyzed using LabSpec 6 Spectroscopy Suite software.

Isotope sampling

Carbonate powders (50–120 µg) for $\delta^{13}C_{shell}$ and $\delta^{18}O_{shell}$ were taken by manual surface micromilling (Fig. 6) using a Rexim Minimo drill with a 300 µm diameter conical SiC drill bit (Gebr. Brasseler GmbH & Co. KG, model number H52 104 003). Samples were drilled parallel to the growth lines from the aperture to the apex (3^{rd}–4^{th} whorl) and taken sequentially at mostly equidistant intervals of approximately 0.5–1.5 mm (Fig. 6). In general, as many samples as possible were taken from each shell (min. 2; max. 100 samples per shell)[39].

Isotope analysis

Stable isotope measurements were carried out at the Institute of Geosciences, University of Mainz. Carbonate powders were dissolved in phosphoric acid at 72 °C in He-flushed exetainers. CO_2 measurements were made using a Thermo Fisher Scientific MAT 253 isotope ratio mass spectrometer operated in continuous flow mode and coupled to a Gas Bench II. Data were calibrated against a Carrara marble supplied by IVA Analysensysteme GmbH ($\delta^{18}O$ = - 1.91‰, $\delta^{13}C$ = + 2.01‰) and NBS-18 ($\delta^{18}O$ = - 23.20‰, $\delta^{13}C$ = - 5.014‰). The reference material IAEA-603 ($\delta^{18}O$ = - 2.37 ‰, $\delta^{13}C$ = + 2.46‰) was used as a quality control standard. The values were reported relative to the VPDB (Vienna-Pee Dee Formation Belemnite) international standard, in per mil (‰). The analytical errors of the instrument (based on 8 injections per sample) were within 0.03 ‰ for $\delta^{13}C$ and 0.06% for $\delta^{18}O$.

Dating

For radiocarbon dating, the shells were treated with diluted hydrochloric acid (1%) to remove contamination attached to the shell. After drying, the CO_2 was extracted in an autosampler using 85% phosphoric acid and the evolving gas transferred to a graphitization system (AGE3, Ionplus). Here, the elemental carbon was reduced with hydrogen gas and iron powder as catalyst. The carbon was then pressed into an aluminum target and measured in a MICADAS type AMS system at Curt Engelhorn Center Archaeometry (CEZA), Mannheim[53]. The samples were calibrated in OxCal 4.4 using the IntCal20 dataset[72,73] without taking a possible hardwater effect into account[53,74,75]. In the figures, ages are presented as the mean value of the two-standard deviation (2σ) date range. The error bars indicate the two absolute 2σ values (minimum and maximum) of the shell. All ages are summarized in the open access data publication, section S41[39].

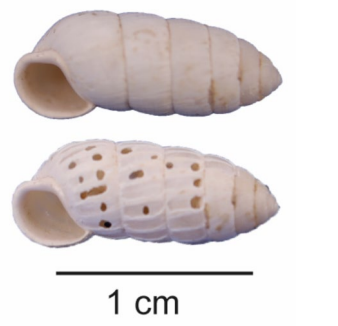

Fig. 6. *Z. insularis* snail (U921) before (left) and after sampling (right) modified after Schmitt and Beuzen-Waller et al.[31].

Classification of the high-resolution shell data

The high-resolution patterns were classified into six categories[31]: (1) Type 2 A: Six snails showed steadily increasing $\delta^{18}O_{shell}$ values. The individual isotope ranges were highly variable, fluctuating between - 2.2‰ and - 0.7‰ (U17) and - 6.4‰ to + 5.0‰ (U2277; Fig. 7A). (2) Type 2 B: Five shells exhibited a steady signal similar to those from (1), but with a decrease in the $\delta^{18}O_{shell}$ values. The individual isotope ranges obtained were highly variable, dropping e.g., from + 1.3‰ to - 11.1‰ (U2337-Z; Fig. 7B). (3) Type 2 C: Eighteen shells showed a sharp drop of up to - 10.4 ‰ in the $\delta^{18}O_{shell}$ values (U503; Fig. 7C). Subsequently, the data slowly increased to reach the previously obtained level. (4) Type 2 D: In thirty-two snails the $\delta^{18}O_{shell}$ values increased continuously before reaching the peak and then continuously decreased (U29; Fig. 7D). This cyclic pattern was observed at least twice during the high-resolution data set, but the width and height of the curve varied greatly, not only between different shells but also within an individual snail. (5) Type 2 E: Two snails showed a rapid change

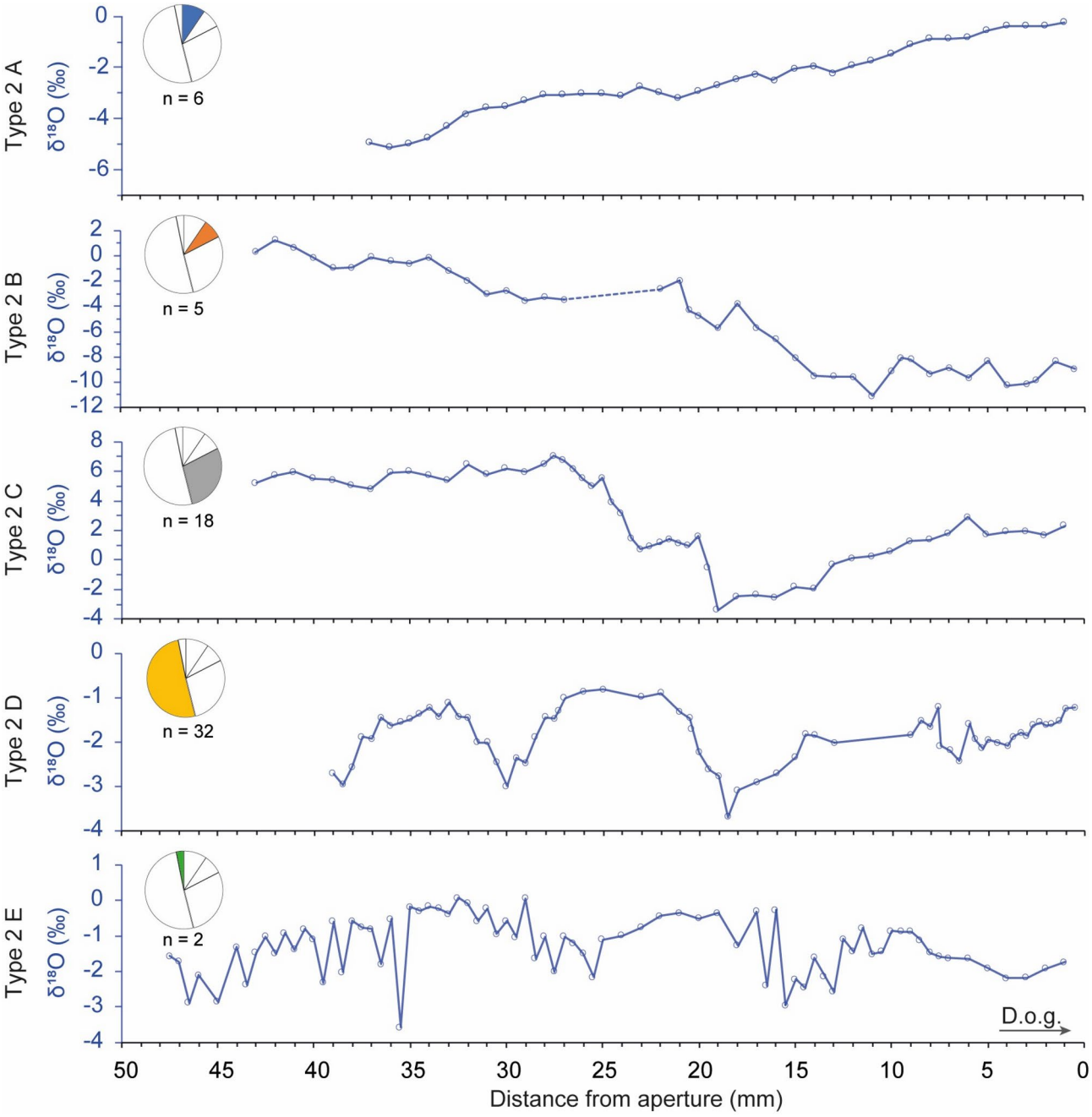

Fig. 7. Examples of the five $\delta^{18}O_{shell}$ patterns classified by Schmitt & Beuzen-Waller et al.[31]. Type 2 A: continuously increasing $\delta^{18}O$ values; Type 2 B: continuously decreasing $\delta^{18}O$ values; Type 2 C: sharp dropping $\delta^{18}O$ values followed by slowly increasing values; Type 2 D: cyclic repetition of alternating minima and maxima and Type 2 E: rapid and sharp change between two adjacent $\delta^{18}O$ values. The pie chart illustrates the occurrence of this pattern in all shells, excluding 23 shells with insufficient measurements to identify a pattern.

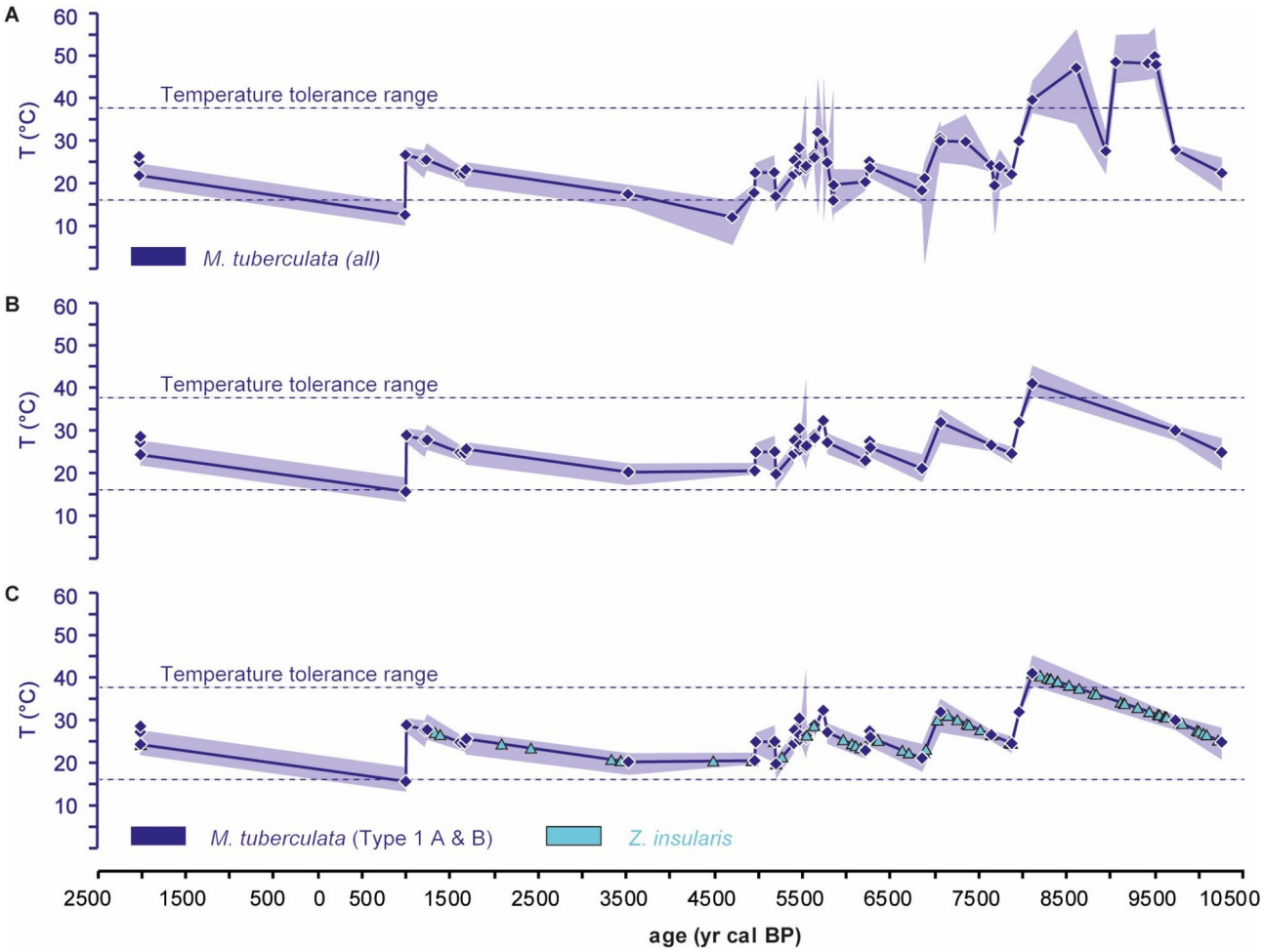

Fig. 8. (**A**) Calculated temperatures range from all aquatic *M. tuberculata* snails (diamonds). (**B**) Calculated temperatures range from the aquatic *M. tuberculata* snails were classified as Type 1 A and B[31]. (**C**) Interpolated temperatures for the *Z. insularis* specimens (triangles) examined in this study. Shaded areas show the minimum and maximum values of the individual snails.

between two adjacent $\delta^{18}O$ values, which vary by up to 1‰. However, this pattern only occurs in certain areas (U921; Fig. 7 E). (6) No signal: Twenty-three snails were sampled with five or fewer data points and therefore not classified in the aforementioned categories because it was not possible to discern a pattern. Further information regarding the isotopic data of the snail shells, their position in the stratigraphic profiles, and their ages can be found in the open access data publication[39].

Integration of shell data

Paleotemperatures recorded by *Melanoides tuberculata*[39] were calculated using the palaeothermometry equation of Grossman and Ku[76], with the VPDB-VSMOW scale correction of - 0.27‰[77,78] and a $\delta^{18}O_{water}$ value of - 1.17‰ (see[39], S42).

$$T_{\delta^{18}O}\,[^{\circ}C] = 20.60 - 4.34 \times \left(\delta^{18}O_{shell} - \left(\delta^{18}O_{water} - 0.27\right)\right) \quad (1)$$

A detailed description of the methodology can be found in Schmitt and Beuzen-Waller et al.[31,39].

A plot of all the aquatic data with their minimum and maximum values (shaded area) reveals that some snails exhibited values outside their temperature tolerance range between 16 and 37 °C (Fig. 8A)[79]. As it is implausible that the snails calcified outside their temperature tolerance range, all the snails identified by Schmitt and Beuzen-Waller et al.[31] as Type 1 C were excluded as they are linked to an open aquatic environment. Instead, only those shells classified as recording a groundwater signal (Type 1 A and B) were included in the subsequent analysis (Fig. 8B). Subsequently, their temperatures were interpolated to align with the ages of the terrestrial snails (Fig. 8C). Due to the lack of available data from sources prior to 10,291–10,194 year cal BP, the data from the seven older snails (10,485–10,247 to 13,599–13,478 year cal BP) were not considered in the $\delta^{18}O_{water}$ reconstruction.

To reconstruct the stable oxygen isotope signature of the water used for the terrestrial shell formation (Fig. 4, $\delta^{18}O_{water;}$ ×), which is assumed to be derived from precipitation-induced moisture, the Grossman and Ku formula was solved for $\delta^{18}O_{water}$[80] using the interpolated temperatures described above (Fig. 8C).

$$\delta^{18}O_{water} = \frac{19.43 - 4.34 \times \delta^{18}O_{shell} - T\,[^{\circ}C]}{-4.34} \quad (2)$$

The $\delta^{18}O_{shell}$ data were presented in δ-notation relative to the Vienna Pee Dee Belemnite (VPDB), while $\delta^{18}O_{water}$ data were presented in δ-notation relative to the Vienna Standard Mean Ocean Water (VSMOW).

Data availability

All data pertaining to the project are stored in an open access WebGIS (https://www.umweltwandel.online/webgis/). Further information regarding the isotopic data of the snail shells, their position in the stratigraphic profiles, and further information has previously been uploaded to Zenodo (https://doi.org/10.5281/zenodo.13341949).

Received: 31 October 2024; Accepted: 9 April 2025
Published online: 21 April 2025

References

1. Tian, Y. et al. Holocene climate change in southern Oman deciphered by speleothem records and climate model simulations. *Nat. Commun.* **14**, 4718. https://doi.org/10.1038/s41467-023-40454-z (2023).
2. Fleitmann, D. et al. Holocene ITCZ and Indian monsoon dynamics recorded in stalagmites from Oman and Yemen (Socotra). *Quat. Sci. Rev.* **26**, 170e188. https://doi.org/10.1016/j.quascirev.2006.04.012 (2007).
3. Fleitmann, D. et al. Droughts and societal change: The environmental context for the emergence of Islam in late Antique Arabia. *Science* **376**, 1317–1321 (2022).
4. Fleitmann, D., Burns, S. J., Matter, A., Cheng, H. & Affolter, S. Moisture and seasonality shifts recorded in Holocene and Pleistocene speleothems from southeastern Arabia. *Geophys. Res. Lett.* **49**, e2021GL097255. https://doi.org/10.1029/2021gl097255 (2022).
5. Fleitmann, D. & Matter, A. The speleothem record of climate variability in Southern Arabia. *Comptes Rendus. Géoscience* **341**, 633–642 (2009).
6. Neff, U. et al. Strong coherence between solar variability and the monsoon in Oman between 9 and 6 kyr ago. *Nature* **411**, 290–293 (2001).
7. Atkinson, O. A. C., Thomas, D. S. G., Goudie, A. S. & Bailey, R. M. Late Quaternary chronology of major dune ridge development in the northeast Rub' al-Khali, United Arab Emirates. *Quat. Res.* **76**, 93–105 (2011).
8. Kocurek, G. et al. Aeolian dune accommodation space for Holocene Wadi Channel Avulsion Strata, Wahiba Dune Field, Oman. *Sediment. Geol.* **399**, 105612. https://doi.org/10.1016/j.sedgeo.2020.105612 (2020).
9. Leighton, C. L., Bailey, R. M. & Thomas, D. S. The utility of desert sand dunes as Quaternary chronostratigraphic archives: evidence from the northeast Rub'al Khali. *Quat. Sci. Rev.* **78**, 303–318 (2013).
10. Preusser, F., Radies, D., Driehorst, F. & Matter, A. Late Quaternary history of the coastal Wahiba sands, Sultanate of Oman. *J. Quat. Sci.* **20**, 395–405 (2005).
11. Berger, J. F. Rivers of the Hadramawt watershed (Yemen) during the Holocene: Clues of late functioning. *Quat. Int.* **266**, 142–161 (2012).
12. Beuzen-Waller, T. et al. Late Pleistocene-Holocene fluvial records of the Wadi Dishshah: hydro-climatic and archaeological implications (Southern piedmont of the Hajar Mountains, Oman). *Géomorphol. Relief Processus Environ.* **28**, 223–239 (2022).
13. Mueller, D. Luminescence chronology of fluvial and aeolian deposits from the Emirate of Sharjah. *UAE. Quat. Res.* **112**, 1–17. https://doi.org/10.1017/qua.2022.51 (2022).
14. Woor, S., Thomas, D. S. G., Durcan, J. A., Burrough, S. L. & Parton, A. The aggradation of alluvial fans in response to monsoon variability over the last 400 ka in the Hajar Mountains, south-east Arabia. *Quat. Sci. Rev.* **322**, 108384. https://doi.org/10.1016/j.quascirev.2023.108384 (2023).
15. Parker, A. G. et al. A record of Holocene climate change from lake geochemical analyses in southeastern Arabia. *Quat. Res.* **66**, 465–476 (2006).
16. Pietsch, D. & Kühn, P. Response of pedogenesis to Holocene climate change in Southern Arabia. In *19th World Congress of Soil Science: Soil Solutions for a Changing World, Brisbane, Australia*. 43–46 (2010).
17. Pietsch, D. et al. Holocene soils and sediments around Ma'rib Oasis, Yemen: further Sabaean treasures?. *Holocene* **20**, 785–799 (2010).
18. Radies, D., Hasiotis, S. T., Preusser, F., Neubert, E. & Matter, A. Paleoclimatic significance of Early Holocene faunal assemblages in wet interdune deposits of the Wahiba Sand Sea, Sultanate of Oman. *J. Arid Environ.* **62**, 109–125 (2005).
19. Matter, A., Neubert, E., Preusser, F., Rosenberg, T. & Al-Wagdani, K. Palaeo-environmental implications derived from lake and sabkha deposits of the southern Rub'al-Khali, Saudi Arabia and Oman. *Quat. Int.* **382**, 120–131 (2015).
20. Parker, A. G. et al. Holocene vegetation dynamics in the northeastern Rub 'al-Khali desert, Arabian Peninsula: a phytolith, pollen and carbon isotope study. *J. Quat. Sci.* **19**, 665–676 (2004).
21. Preston, G. W. et al. A multi-proxy analysis of the Holocene humid phase from the United Arab Emirates and its implications for southeast Arabia's Neolithic populations. *Quat. Int.* **382**, 277–292 (2015).
22. Lézine, A. M., Saliege, J. F., Robert, C., Wertz, F. & Inizan, M. L. Holocene lakes from Ramlat as-Sab'atayn (Yemen) illustrate the impact of monsoon activity in southern Arabia. *Quat. Res.* **50**, 290–299 (1998).
23. Lézine, A. M. et al. Centennial to millennial-scale variability of the Indian monsoon during the early Holocene from a sediment, pollen and isotope record from the desert of Yemen. *Palaeogeogr. Palaeoclimatol. Palaeoecol.* **243**, 235–249 (2007).
24. Lézine, A. M. et al. Climate change and human occupation in the Southern Arabian lowlands during the last deglaciation and the Holocene. *Glob. Planet. Change* **72**, 412–428 (2010).
25. Urban, B. & Buerkert, A. Palaeoecological analysis of a Late Quaternary sediment profile in northern Oman. *J. Arid Environ.* **73**, 296–305 (2009).
26. Leng, M. J., Heaton, T. H., Lamb, H. F. & Naggs, F. Carbon and oxygen isotope variations within the shell of an African land snail (*Limicolaria kambeul chudeaui* Germain): a high-resolution record of climate seasonality?. *Holocene* **8**, 407–412 (1998).
27. Zong, X. et al. Precipitation $\delta^{18}O$ paced the seasonal $\delta^{18}O$ variations of terrestrial snail body water and shells in the East Asian monsoon region. *Quat. Sci. Rev.* **317**, 108290. https://doi.org/10.1016/j.quascirev.2023.108290 (2023).
28. Wang, G. et al. Quantitative reconstruction of a single super rainstorm using daily resolved $\delta^{18}O$ of land snail shells. *Sci. Bull.* **69**, 2281–2288 (2024).
29. Prendergast, A. L., Stevens, R. E., Barker, G. & O'Connell, T. C. Oxygen isotope signatures from land snail (*Helix melanostoma*) shells and body fluid: proxies for reconstructing Mediterranean and North African rainfall. *Chem. Geol.* **409**, 87–98 (2015).

30. Schmitt, K. E., Walliser, E. O., Schöne, B. R., Gey, C. J. & Schmidt, C. Environmental reconstructions based on aquatic and terrestrial snails originating from the Early Bronze Age and the Late Islamic Period–A stable isotope case study from the Al-Khashbah archaeological Site, Sultanate of Oman. *J. Archaeol. Sci. Rep.* **45**, 103620. https://doi.org/10.1016/j.jasrep.2022.103620 (2022).
31. Schmitt, K. E. et al. *Melanoides tuberculata* and *Zootecus insularis* gastropod shells provide a snapshot into past hydroclimatic conditions of arid environments: New perspectives from Oman. *Palaeogeogr. Palaeoclimatol. Palaeoecol.* **655**, 112542. https://doi.org/10.1016/j.palaeo.2024.112542 (2024).
32. Dong, J. et al. Ultra-high resolution $\delta^{18}O$ of land snail shell: A potential tool to reconstruct frequency and intensity of paleoprecipitation events. *Geochim. Cosmochim. Acta* **327,** (2022).
33. Cremaschi, M. et al. Early-Middle Holocene environmental changes and pre-Neolithic human occupations as recorded in the cavities of Jebel Qara (Dhofar, southern Sultanate of Oman). *Quat. Int.* **382**, 264–276 (2015).
34. Weyhenmeyer, C. E. et al. Cool glacial temperatures and changes in moisture source recorded in Oman groundwaters. *Science* **287**, 842–845 (2000).
35. Weyhenmeyer, C. E., Burns, S. J., Waber, H. N., Macumber, P. G. & Matter, A. Isotope study of moisture sources, recharge areas, and groundwater flow paths within the eastern Batinah coastal plain, Sultanate of Oman. *Water Resour. Res.* **38**, 1184. https://doi.org/10.1029/2000WR000149 (2002).
36. Dansgaard, W. Stable isotopes in precipitation. *Tellus* **16**, 436–468 (1964).
37. Burns, S. J., Matter, A., Frank, N. & Mangini, A. Speleothem-based paleoclimate record from northern Oman. *Geology* **26**, 499–502 (1998).
38. Fleitmann, D. et al. Holocene records of rainfall variation and associated ITCZ migration from stalagmites from Northern and Southern Oman. In *The Hadley Circulation: Present, Past and Future. Advances in Global Change Research*, vol. 21 (eds. Diaz, H. F. and Bradley, R. S.) 259–287 (Springer, 2004).
39. Schmitt, K. E. Supplementary data. Zenodo https://doi.org/10.5281/zenodo.13341949 (2024).
40. Lachniet, M. S. Climatic and environmental controls on speleothem oxygen-isotope values. *Quat. Sci. Rev.* **28**, 412–432 (2009).
41. Rech, J. A. et al. Assessing open-system behavior of ^{14}C in terrestrial gastropod shells. *Radiocarbon* **53**, 325–335 (2011).
42. Fohlmeister, J. et al. Main controls on the stable carbon isotope composition of speleothems. *Geochim. Cosmochim. Acta* **279**, 67–87 (2020).
43. Stott, L. D. The influence of diet on the $\delta^{13}C$ of shell carbon in the pulmonate snail *Helix aspersa*. *Earth Planet. Sci. Lett.* **195**, 249–259 (2002).
44. McConnaughey, T. A. & Gillikin, D. P. Carbon isotopes in mollusk shell carbonates. *Geo-Mar. Lett.* **28**, 287–299 (2008).
45. Hassan, K. M. The stable isotopes of modern land snail shell from Sinn El-Kedab plateau, southwest Aswan, Egypt. *Isot. Radiat. Res.* **38**, 107–116 (2006).
46. Lécuyer, C. et al. $\delta^{18}O$ and $\delta^{13}C$ of diagenetic land snail shells from the Pliocene (Zanclean) of Lanzarote, Canary Archipelago: Do they still record some climatic parameters?. *J. Afr. Earth Sci.* **162**, 103702. https://doi.org/10.1016/j.jafrearsci.2019.103702 (2020).
47. Rudov, A., Mashkour, M., Djamali, M. & Akhani, H. A review of C4 plants in southwest Asia: an ecological, geographical and taxonomical analysis of a region with high diversity of C4 eudicots. *Front. Plant Sci.* **11**, 546518. https://doi.org/10.3389/fpls.2020.546518 (2020).
48. Swerida, J. et al. Cultural and human ecological resilience at Early Bronze Age Bat. *Open Quat.* **10**, 7. https://doi.org/10.5334/oq.150 (2024).
49. Proctor, L., Döpper, S. & Schmidt, C. Hafit period fuelwood preferences associated with early copper production at Building V, al-Khashbah, Oman. *Proc. Semin. Arab. Stud.* **53**, 230–247 (2024).
50. Deckers, K., Döpper, S. & Schmidt, C. Vegetation, land, and wood use at the sites of Bat and Al-Khashbah in Oman (fourth–third millennium BC). *Arab. Archaeol. Epigr.* **30**, 1–14 (2019).
51. Döpper, S. Walk the line: the 2020 field season of the Al-Mudhaybi Regional Survey. *Proc. Semin. Arab. Stud.* **51**, 157–167 (2022).
52. Girod, A. & Sassoon, D. Distribution and ecology of *Zootecus insularis* (Ehrenberg, 1831) (Gastropoda, Pulmonata, Achatinidae, Subulininae) and its value as a palaeoenvironmental indicator species. *Basteria*. (2022).
53. Lindauer, S. et al. Investigating the local reservoir age and stable isotopes of shells from southeast Arabia. *Radiocarbon* **59**, 355–372 (2017).
54. Philippsen, B. The freshwater reservoir effect in radiocarbon dating. *Herit. Sci.* **1**, 1–19 (2013).
55. Matter, J. M., Waber, H. N., Loew, S. & Matter, A. Recharge areas and geochemical evolution of groundwater in an alluvial aquifer system in the Sultanate of Oman. *Hydrogeol. J.* **14**, 203–224 (2006).
56. Loges, L. Leben mit dem Verschwinden des Wassers—Wie Menschen in der Bronzezeit mit Umweltveränderungen umgingen. *Antike Welt* **2**(24), 46–55 (2024).
57. Schmidt, C. & Döpper, S. The Hafit period at Al-Khashbah, Sultanate of Oman: Results of four years of excavations and material studies. *Proc. Semin. Arab. Stud.* **49**, 265–274 (2019).
58. Schmidt, C., Döpper, S., Ochs, U., Petrella, S., & Kluge, J. *Die Entstehung komplexer Siedlungen im Zentraloman: Archäologische Untersuchungen zur Siedlungsgeschichte von Al-Khashbah* (Archaeopress, 2021)
59. Döpper, S. Survey methods and biases in the Al-Mudhaybi Regional Survey, Sultanate of Oman. *Arab. Archaeol. Epigr.* **34**, S39–S50 (2023).
60. Döpper, S. & Schmidt, C. Nothing but tombs and towers? Results of the Al-Mudhaybi Regional Survey 2019. *Proc. Semin. Arab. Stud.* **50**, 157–170 (2020).
61. Biezeveld, I. Re (dis) covering the recent: Surveying settlements and society in central Oman from the 17th to the 20th centuries. *Arab. Archaeol. Epigr.* **34**, S107–S121 (2023).
62. Climate Change Knowledge Portal. https://climateknowledgeportal.worldbank.org/country/oman/climate-data-historical (2024).
63. Ghazanfar, S. A. *Flora of the Sultanate of Oman. Volume 1. Piperaceae—Primulaceae. Scripta Botanica Belgica 25* (Botanic Garden Meise, 2003).
64. Patzelt, A. Synopsis of the flora and vegetation of Oman, with special emphasis on patterns of plant endemism. *Abhandlungen Der Braunschweigischen Wissenschaftlichen Gesellschaft*. 282–317 (2015).
65. Balakrishnan, M. & Yapp, C. J. Flux balance models for the oxygen and carbon isotope compositions of land snail shells. *Geochim. Cosmochim. Acta* **68**, 2007–2024 (2004).
66. Qamar, S. U. R., Saif, A. & Altaf, J. Identification of the species of genus Zootecus on the basis of morphology. *J. Biodivers. Environ. Sci.* **11**, 122–127 (2017).
67. Feulner, G. R. & Green, S. A. Terrestrial molluscs of the United Arab Emirates. Mitt. dtsch. malakozool. *Ges* **69**, 23–34 (2003).
68. Neubert, E. The continental malacofauna of Arabia and adjacent areas, II. The genus Zootecus Westerlund 1887 (Gastropoda: Pulmonata: Subulinidae). *Archiv für Molluskenkunde* **132**, 153–160 (2003).
69. Kiwan, K. et al. *Terrestrial environments of Abu Dhabi Emirate, UAE* (Environment Agency—Abu Dhabi, 2008).
70. Al-Khayat, J. A. First record of five terrestrial snails in the State of Qatar. *Turk. J. Zool.* **34**, 539–545 (2010).
71. Neubert, E. Annotated checklist of the terrestrial and freshwater molluscs of the Arabian Peninsula with description of new species. *Fauna of Arabia* **17**, 333–461 (1998).
72. Ramsey, C. B. Radiocarbon calibration and analysis of stratigraphy: the OxCal program. *Radiocarbon* **37**, 425–430 (1995).
73. Reimer, P. J. Composition and consequences of the IntCal20 radiocarbon calibration curve. *Quat. Res.* **96**, 22–27 (2020).

74. Lindauer, S., Milano, S., Steinhof, A. & Hinderer, M. Heating mollusc shells-A radiocarbon and microstructure perspective from archaeological shells recovered from Kalba, Sharjah Emirate, UAE. *J. Archaeol. Sci. Rep.* **21**, 528–537 (2018).
75. Lindauer, S. Radiocarbon reservoir effects on shells from SE Arabia in the context of paleoenvironmental studies. *Doctoral dissertation, Technical University of Darmstadt* (2019).
76. Grossman, E. L. & Ku, T. L. Oxygen and carbon isotope fractionation in biogenic aragonite: temperature effects. *Chem. Geol. Isotope Geosci. Sect.* **59,** 59–74 (1986).
77. Gonfiantini, R., Stichler, W., & Rozanski, K. Standards and intercomparison materials distributed by the International Atomic Energy Agency for stable isotope measurements (IAEA-TECDOC–825). International Atomic Energy Agency (IAEA) (1995).
78. Dettman, D. L., Reische, A. K. & Lohmann, K. C. Controls on the stable isotope composition of seasonal growth bands in aragonitic fresh-water bivalves (Unionidae). *Geochim. Cosmochim. Acta* **63**, 1049–1057 (1999).
79. Okumura, D. T. & Rocha, O. Life history traits of the exotic freshwater snail *Melanoides tuberculata* Müller, 1774 (Gastropoda, Thiaridae), and its sensitivity to common stressors in freshwaters. *Acta Limnol. Bras.* **32**, e19. https://doi.org/10.1590/s2179-975x0819 (2020).
80. Schöne, B. R. et al. Freshwater pearl mussels from northern Sweden serve as long-term, high-resolution stream water isotope recorders. *Hydrol. Earth Syst. Sci.* **24**, 673–696 (2020).

Acknowledgements

We thank Michael Maus (JGU Mainz), Anka Carina Meßmer (JGU Mainz) and Leonie Lange (University of Potsdam) for laboratory assistance, Lukas Fröhlich (JGU Mainz) for the interpolation tool program. Financial support from the German Federal Ministry of Education and Research (BMBF) with funding reference numbers 01UL2001A–D is gratefully acknowledged.

Author contributions

K.E.S. conducted laboratory work, was responsible for the analysis of the data, prepared Figs. 2, 3, 4, 5, 6, 7 and 8, wrote the main manuscript. L.P. collected samples and wrote the main manuscript. T. B.-W. collected samples and provided essential environmental data. C.S. was responsible for the organization of the project on site and prepared Fig. 1. S.L. performed AMS analysis. M.J., M.P.M., M.S., J.S., S.P. provided samples from their respective projects and gave important information about the sampling sites. B.R.S. conducted laboratory work. All authors reviewed and edited the manuscript.

Competing interests

The authors declare no competing interests.

Additional information

Correspondence and requests for materials should be addressed to K.E.S. or L.P.